Journal of Materials Processing Tech. 273 (2019) 116192

Contents lists available at ScienceDirect

Journal of Materials Processing Tech.

journal homepage: www.elsevier.com/locate/jmatprotec

Combining resistance spot welding and friction element welding for dissimilar joining of aluminum to high strength steels

J.P. Oliveira[a,b,*], K. Ponder[b], E. Brizes[b], T. Abke[c], P. Edwards[d], A.J. Ramirez[b,**]

[a] UNIDEMI, Departamento de Engenharia Mecânica e Industrial, Faculdade de Ciências e Tecnologia, Universidade NOVA de Lisboa, Caparica, Portugal
[b] Welding Engineering, Department of Materials Science and Engineering, The Ohio State University, 1248 Arthur E. Adams Drive, Columbus, OH, 43221, USA
[c] Honda R&D Americas, North America, 21001 State Route 739, Raymond, OH, 43067, USA
[d] Honda Engineering North America, Inc. 24000 Honda Parkway, Marysville, OH 43040, USA

ARTICLE INFO

Associate Editor: C.H. Caceres

Keywords:
High strength steels
Usibor 1500
Aluminum alloys
Resistance spot welding
Friction element welding
Mechanical testing

ABSTRACT

A multi-process joining technique that combined resistance spot welding and friction element welding was used to produce a three-sheet multi-stack of advanced high strength steel and precipitation hardened aluminum. Each weld process was tested independently and as a combination to better understand how multi-step welding affects joint performance. Weld interfaces and surrounding heat affected zones were investigated using microstructural and mechanical techniques, including scanning electron microscopy and nanoindentation. All tests indicated that excellent strength was maintained above the maximum breaking force threshold regardless of offset distance between the friction element weld and the center of the resistance spot weld nugget. A change in fracture mode was observed with interfacial fracture occurring at offset distances below 7 mm and nugget pull out or partial thickness failure occurred at offset distances above 7 mm. The present study indicates that hybrid joining techniques have minimal effect on both the mechanical and microstructural weld properties and allow for new dissimilar metal weld designs to be implemented in the automotive industry.

1. Introduction

Resistance spot welding of Usibor is widely performed both by independent researchers and industry: Ighodaro et al. (2016) joined Al-Si coated and galvannealed steels and found that the coating significantly impacts the welding parameters; Eller et al. (2015) have developed material models to predict the plastic behavior in the different thermally affected regions of resistance spot welded high strength steel. Resistance spot welding promotes joining due to the generation of heat created by the application of an electrical current through a joint. This heat generation should be substantial enough to promote local melting and the formation of a nugget at the interface of the two joining materials. The amount of heating that can be generated during the process is usually limited by the electrical conductivity of the materials to be joined, with lower electrical conductivity enabling the generation of more heat. Moreover, such process may be greatly influenced by the material's surface condition. Resistance spot welding occurs during a given cycle time and the welding current, welding time and electrode force are the most important process parameters. According to Boriwal et al. (2017), the cooling rate experienced by the welded joint will depend on the material thickness and can range from around 100 °C/s to 3000 °C/s, with a potential increase due to the use of water-cooled electrodes.

Joining of three or more sheets of material (multi-stacks) using resistance spot welding is difficult due to the challenges associated with determining the optimal process parameters. Furthermore, if dissimilar materials are to be joined in the multi-stack (e.g., high strength steels and low-density alloys), resistance spot welding process development increases in complexity. Differences in material properties (e.g., electrical conductivity, thermal conductivity, melting temperature and thickness) alter the heat balance required for proper nugget formation. The tortuous experimental process necessary for multi-stack parameter development has pushed the automotive industry to consider multi-process joining.

To achieve sound welds in multi-stack joining, combining different joining technologies is fundamental for success. Therefore, one must

* Corresponding author at: UNIDEMI, Departamento de Engenharia Mecânica e Industrial, Faculdade de Ciências e Tecnologia, Universidade NOVA de Lisboa, Caparica, Portugal.
** Corresponding author at: Welding Engineering, Department of Materials Science and Engineering, The Ohio State University, 1248 Arthur E. Adams Drive, Columbus, OH, 43221, USA.
E-mail addresses: jp.oliveira@fct.unl.pt (J.P. Oliveira), ramirez.49@osu.edu (A.J. Ramirez).

https://doi.org/10.1016/j.jmatprotec.2019.04.018
Received 29 January 2019; Received in revised form 27 March 2019; Accepted 10 April 2019
Available online 12 April 2019
0924-0136/

Table 1
Chemical composition of Usibor 1500 press hardened steel.

Element (wt. %)	C	Mn	P	S	Si	Al	Ni	Cr	Ti	Cu	N	B	Fe
	0.21	1.22	0.013	0.001	0.265	0.056	0.01	0.19	0.033	0.01	0.0052	0.0031	Balance

pay attention to the material combinations being joined and whether they are the most suitable joining techniques that can be used, while also keeping in mind production costs and efficiency. In particular, for the case of multi-stack joining of high strength steels to aluminum alloys for the automotive industry, one must pay attention to industry requirements that include: safe and mechanically sound joints, with high production rates, low process variability and low cost.

Friction element welding is a relatively new technique used to join overlapped parts. In this technique, heat is generated purely by mechanical effects: frictional heating under rotational relative movement and force which is being applied to the surfaces being joined. As stated by Maiwald and Thiem (2012), the process occurs in the solid state and the frictional heating created by the element plasticizes the material, creating a radial displacement of material promoting joining and at the same time a self-cleaning effect.

There are four steps in friction element welding: penetration, cleaning, welding and compression. In the penetration step, the frictional heating generated on the top surface between the friction element weld and the softer sheet, (aluminum in this case) allows the material to flow upwards. This material flow creates a flash which is collected underneath the head of the friction element. The specific head design of the friction element weld accommodates the displacement of the aluminum during this initial step. The cleaning step is required to remove any coating that may exist between the materials being joined. This step starts when the head of the friction element touches the high strength steel. At that point, the combined effect of temperature and high rotational speed removes any coating and/or impurities, creating a clean surface. The cleaning aspect of the process is especially relevant for the automotive industry, where handled materials are often provided with non-ideal conditions for welding due to the presence of contaminants and debris.

Next, welding is initiated during the third step. The axial force is amplified thus increasing the frictional heating. This increase in frictional heating promotes softening of the high strength steel and of the friction element in the area to be joined. At this point a friction weld is created. An important feature of friction element welding is that the maximum welding temperature is below the liquidus temperature of the high strength steel and friction element. As such, no liquid pool is formed, which decreases the risk of formation of undesired phases such as brittle intermetallic compounds. Finally, in the fourth step, the friction element rotation stops, and the axial force increases. This step intends to close any cracks that were potentially formed as a result of the abrupt stop in rotation. Additionally, such increase in the applied axial load will guarantee that the materials being joined will be in full contact with each other in case such did not occur in the previous steps of the process.

Typical advantages of friction element welding include the possibility to join different materials such as Al, Mg, and steel in double or triple layers. Additionally, this is a low heat input technique, free from distortion that requires no preparation. Finally, during the process the emissions are minimal or even non-existent.

In this work, the combination of resistance spot welding and friction element welding within a three-sheet automotive multi-stack was evaluated. The joint design of interest consisted of two sheets of resistance spot welded hot-stamped boron steel joined to a precipitation hardened aluminum by a friction element weld. Microstructural characterization of the multiple stacks was performed, the effect of the offset distance between the welded nugget and the friction element was seen to influence the mechanical properties of the welded joints. However, the joints were able to sustain higher forces than the welded joints used as a baseline, showing the feasibility of these hybrid techniques to be employed in a wide range of industries, such as automotive. This work combines advanced materials characterization and mechanical testing to understand the effect of each process on the final microstructure and mechanical properties of the Aluminum/Usibor joints.

2. Experimental procedure

2.1. Materials

Usibor 1500 with 1.4 mm thickness was used. Usibor steels have an aluminium-silicon coating, which is used to protect the material from oxidation and decarburization during hot stamping. The chemical composition of the Usibor material is depicted in Table 1. Aluminium 6005-T5 in the extruded condition with a thickness of 2.0 mm was also used. The friction element used has a diameter of 4.55 mm and a length of 5.0 mm and reference EW4-Z-10. The friction element is made of a creep resistant quenched and tempered Cr-Mo steel which is coated with a Zn-Ni layer. The chemical composition of the friction element is presented in Table 2.

2.2. Resistance spot welding

Resistance spot welding was performed using a Medium Frequency Direct Current (MFDC) resistance spot welder equipped with a servo driven force system available at the Edison Joining Technology Center. The weld cycle used is presented in Fig. 1 and Table 3. Note that 1 weld cycle corresponds to 1/60 of a second. Spherical Cu electrodes with 6 mm face dome radii were used while water cooled the electrode.

2.3. Friction element welding

After joining two stacks of Usibor through resistance spot welding, a stack of Aluminum 6005-T5 was joined by friction element welding, using an CFF 38/95V friction welding machine from EJOT.

The weld scheme is composed of four different steps to join the Aluminum to the Usibor stack. The selected four steps vary rotation speed in revolutions per minute (RPM) and force imposed by the friction element, these steps are presented in Table 4.

It is important to explain the different steps used for friction element welding. In the first step, the upper plate (Aluminum) is penetrated by the rotating element at a given speed and with a given axial force which is dependent on the material to be penetrated and its thickness. Then, on the

Table 2
Chemical composition of the friction element used.

Element (wt. %)	C	Mn	P	S	Si	Cr	Ni	Mo	V	Fe
	017-025	0.40-0.80	0.030	0.030	0.4	1.20-1.50	0.60	0.55-0.85	0.20-0.35	Balance

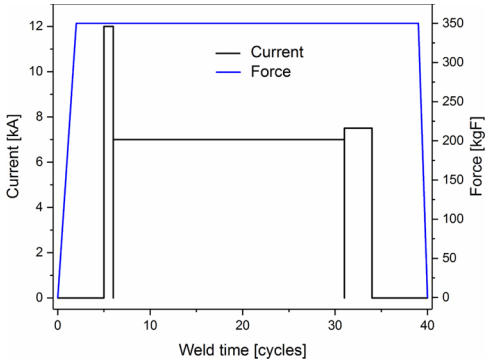

Fig. 1. Weld schedule used for resistance spot welding of 1.4 mm thick Usibor 1500 steel.

Table 3
Process parameters used for resistance spot welding of Usibor 1500 steel.

Step	Weld time [cycles]	Current [kA]	Force [kgf]
Hold	5	0	Ramp to 350
Preheat	12	12	350
Weld	25	7	350
Temper	3	7.5	350
Hold	5	0	Ramp to 0

Table 4
Process parameters used for friction element welding of 2.0 mm thick Aluminum 6005-T5 to 1.4 mm thick Usibor 1500 steel.

Step #	Rotation speed [RPM]	Axial force [kN]	Relative distance [mm]
1	3000	8.0	1.7
2	5500	7.0	2.85
3	6000	8.0	4.0
4	0	9.0	0.2 s

second stage, any existing coatings are removed. On the third stage, the friction element joint is achieved. The fourth stage completes the welding by continuing to apply a given axial force without any rotational speed.

To determine the influence of the friction element position regarding the resistance spot welding nugget several welds were performed varying the offset between the center of the nugget and the center of the friction element. The offset distances analyzed varied between no offset (friction element placed on top of the resistance spot welding nugget) to a maximum of 15 mm, where the friction element was placed on top of the non-affected Usibor material. A schematic representation of this offset distance is presented in Fig. 2 c and d (refer to section 2.5 of the paper).

2.4. Microstructural characterization

The microstructure of the produced joints was analyzed by means of conventional optical microscopy and scanning electron microscopy. The analyzed samples were cross-sectioned and polished up to 1 µm diamond paste using standard metallographic techniques. The final step of polishing used a colloidal silica suspension on a vibratory polisher. To reveal the grain structure of the joint, a 2% Nital etching solution was used.

Optical microscopy was performed using an Olympus GX51 optical microscope and scanning electron microscopy was performed using a FEI Helios NanoLab™ 600 DualBeam SEM with an acceleration voltage of 30 keV.

Vickers microhardness mapping of selected joints was also performed to understand the effect of both processes and their effect on the softening and/or hardening of the two materials. A LECO LM100AT microhardness tester with a load of 300 g and a dwell time of 15 s was used to map regions of interest through the dissimilar joints. The indent

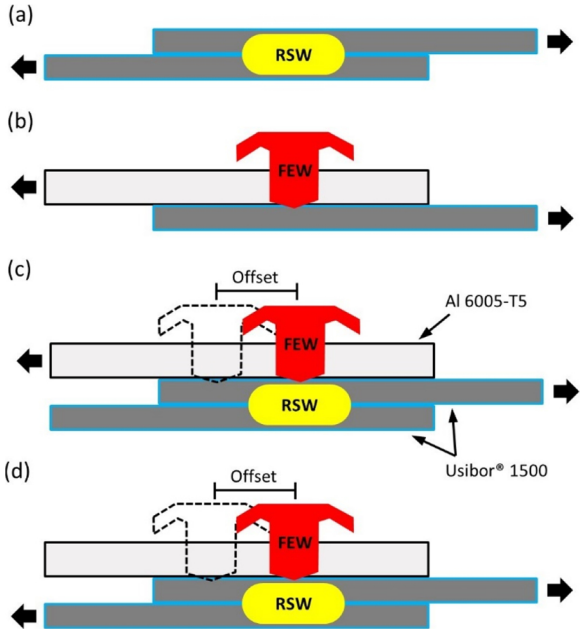

Fig. 2. Schematic representation of the tensile shear tests performed: (a) resistance spot welded steel/steel joint; (b) friction element welded aluminum/steel joint; combined resistance spot weld and friction element weld joint to evaluate the effect of the offset distance on the mechanical performance of the (c) friction element welds and (d) resistance spot welds.

spacing between measurements was 200 µm. Note that all microhardness maps have the same scale to make it possible to compare between each weld configuration studied in this work.

2.5. Mechanical performance

To evaluate the mechanical properties of the multiple stack joints, shear tension tests were performed following the JIS Z 3136 standard. A MTS 810 Material Tests System tensile machine with a load capacity of 100 kN was used. The cross-head displacement was set at 15 mm/min and the initial gauge length was set to 115 mm. The maximum breaking force was recorded for all samples. For a thorough understanding of the effect of the combined use of resistance spot welding and friction element welding on the multiple stack joint, two distinct configurations were tested: the first, to evaluate the mechanical properties of the friction element welded joints; the second, to evaluate the mechanical properties of the resistance spot welded joint. In order to have a baseline for comparison, shear tensile testing of Usibor/Usibor resistance spot welded joints and Usibor/Aluminum 6005-T5 friction element welding joints were also performed. Fig. 2, depicts a schematic representation of the different configurations used to evaluate the effect of both processes on the mechanical properties.

After mechanical testing, the fracture modes experienced by the joints were characterized using optical microscopy and scanning electron microscopy.

3. Results and discussion

3.1. Resistance spot welding microstructural characterization

High magnification images of the resistance spot weld microstructure are presented in Fig. 3. Hardness maps of the resistance spot welded Usibor sheets are depicted in Fig. 4. Due to the distinct heating and cooling rates experienced in different regions of the material, several regions are observed. These regions exhibited different microstructural features and hence different hardness values.

The differences in hardness values are a result of the distinct thermal history experienced by each region. From the metallographic

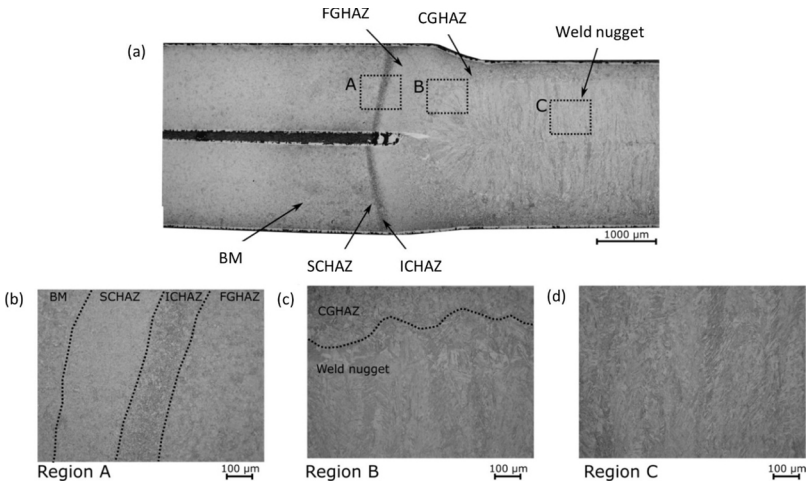

Fig. 3. Resistance spot welded Usibor 1500 microstructure: (a) macrograph; (b) high magnification of region A: base material (BM), subcritical heat affected zone (SCHAZ), intercritical heat affected zone (ICHAZ), and fine-grain heat affected zone (FGHAZ); (c) high magnification of region B: coarse grain heat affected zone (CGHAZ) and the weld nugget; (d) high magnification of region C: weld nugget").

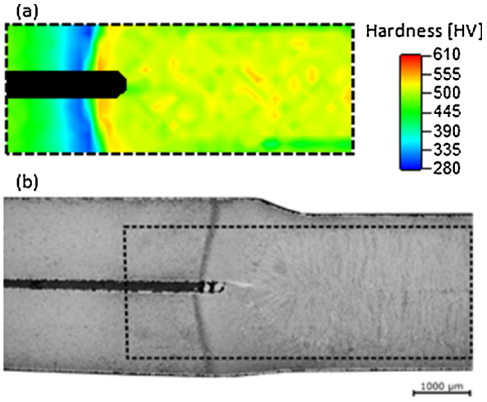

Fig. 4. a) Microhardness map of the Usibor 1500 resistance spot welded joint; (b) macrograph of the resistance spot welded joint with dashed box indicating the indented region.

analysis of the Usibor resistance spot welded stack, six different regions are observed: weld nugget or fusion zone, coarse-grain heat affected zone (CGHAZ), fine-grain heat affected zone (FGHAZ), intercritical heat affected zone (ICHAZ), subcritical heat affected zone (SCHAZ), and base material (BM).

The center of the weld nugget experiences the maximum temperatures during welding (above its liquidus temperature). During resistance spot welding, the copper electrodes are water cooled and act as heat sinks, thus extracting heat from the nugget rapidly. The fast cooling that occurs in the fusion zone promotes epitaxial solidification of a dendritic structure with a directional growth towards the centerline (Fig. 3a). As a result of the fast heat extraction, the weld nugget is quenched. This rapid solidification ensures that austenite fully transforms back to martensite. The highest hardness is achieved within the fusion zone of the welded joint, ranging between 500 and 530 HV. According to Pouranvari and Marashi (2013), all but very lean alloyed steels exhibit a fully martensitic structure due to the fast cooling rates associated with this welding technique.

Adjacent to the weld nugget one can observe the different heat affected regions (Fig. 3a and b). Just after the weld nugget interface, exists the coarse-grain heat affected zone. In this region, the material was kept above the Ac_3 temperature for a significant period, which allowed for the growth of austenite grains at high temperature. The subsequent rapid cooling also associated with this region of the welded joint enabled the austenite to transform into martensite upon cooling. Additionally, the martensitic transformation is aided by the coarser grain size of the austenite grains as described by Khan et al. (2008). In the coarse grain heat affected zone the hardness is about 510 HV, close to that measured on the fusion zone.

The following region is the fine-grain heat affected zone. Here, the peak temperature is still above Ac_3, thus promoting full austenitization. However, the peak temperature and the permanence time is lower than that experienced in the coarse-grain heat affected zone. In the fine-grain heat affected zone the temperature is enough to induce austenite recrystallization, hence the smaller grain size in this region. The next region observed is the intercritical heat affected zone. In this region the peak temperatures range between Ac_1 and Ac_3, that is, in the austenite + ferrite domain. A significant decrease in hardness to around 330 HV occurs in this region. This is related to the presence of ferrite in the microstructure.

Following this step, it comes the subcritical heat affected zone where the maximum temperature reached is bellow Ac_1. This will result in the tempering of martensite and with potential coarsening of carbides. This tempering effect significantly decreases the hardness of this region, when compared to the base material, to 360 HV.

Scanning electron microscopy of each region is presented in Fig. 5 detailing the different microstructures obtained. Fig. 5a depicts the tempered martensitic base material of the Usibor steel. Finely dispersed carbides (cementite) were observed throughout the material. The large martensitic lath microstructure of the fusion zone is depicted in Fig. 5b. In Fig. 5c the microstructure of the FGHAZ (left) and ICHAZ (right) shows the formation of ferrite in the ICHAZ that formed between A1 and A3 temperatures in addition to the over-tempered martensite that formed below A1 temperatures. Fig. 5d depicts the microstructure of the ICHAZ (left) and SCHAZ (right). The subcritical region is composed of over-tempered martensite, where the cementite particles have coarsened from exposure to elevated temperatures.

In resistance spot welding, the cooling rate is governed by the heat dissipation from the fusion zone. Two distinct mechanisms occur: heat dissipation assisted by the electrodes along the axial direction and heat dissipation through the base material along the radial direction. Depending on the thickness of the plates to be welded, and the electrodes used, one mechanism may be favored over the other. As a result of this heat dissipation, the maximum temperatures reached within each different microstructure across the weld will occur as shown before.

3.2. Friction element welding microstructural characterization

The microstructure of a friction element weld obtained between one sheet of aluminum 6005-T5 and one sheet of Usibor 1500 using the

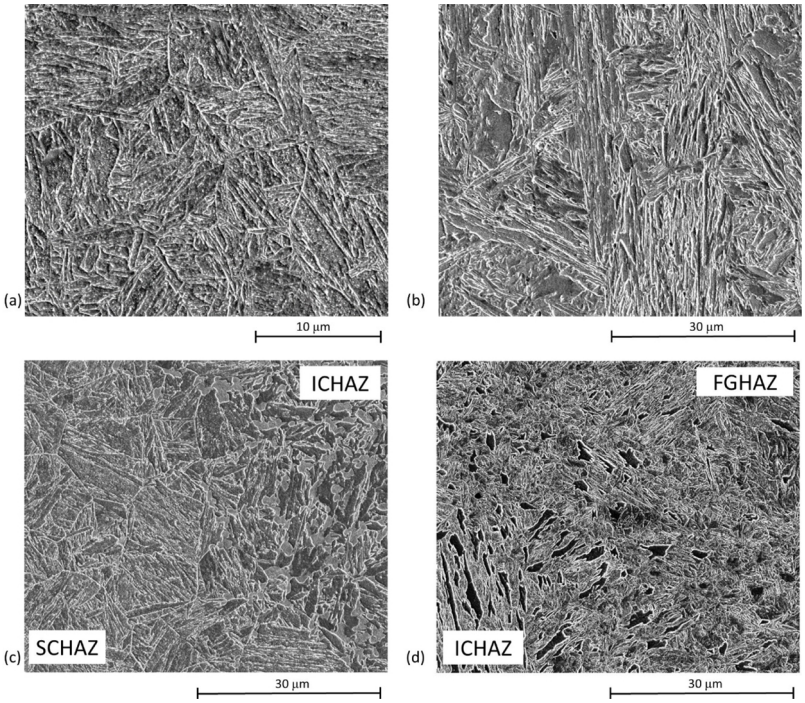

Fig. 5. Usibor 1500 steel RSW microstructures: (a) base material in the press-hardened condition; (b) fusion zone; (c) SCHAZ left and ICHAZ right; (d) ICHAZ left and FGHAZ right.

welding parameters previously shown is depicted in Fig. 6. It can be seen the upward flow of the aluminum flash and how it collects underneath the friction element top. This material flow directed by high rotational speed and pressure applied to the work piece. The rotational displacement of material contributes to the refined martensitic structure visible on both sides of the faying surfaces. Additionally, it can be observed that a very refined martensitic structure is obtained on both sides of the joining interface (Fig. 6a). This decrease in grain size is due to dynamic recrystallization occurring at and near the joining interface. In the intercritical and subcritical heat affected zones the microstructure is similar to that observed in the Usibor resistance spot welded joint.

The microhardness mapping of the friction element weld between the aluminum 6005-T5 and the Usibor sheets is depicted in Fig. 7. It can be observed that the hardness across the interface is slightly higher than in the resistance spot welded nugget previously shown in Fig. 4a. This is attributed to the refined grain size of the material due to dynamic recrystallization and high cooling rate ensuring a complete martensitic transformation.

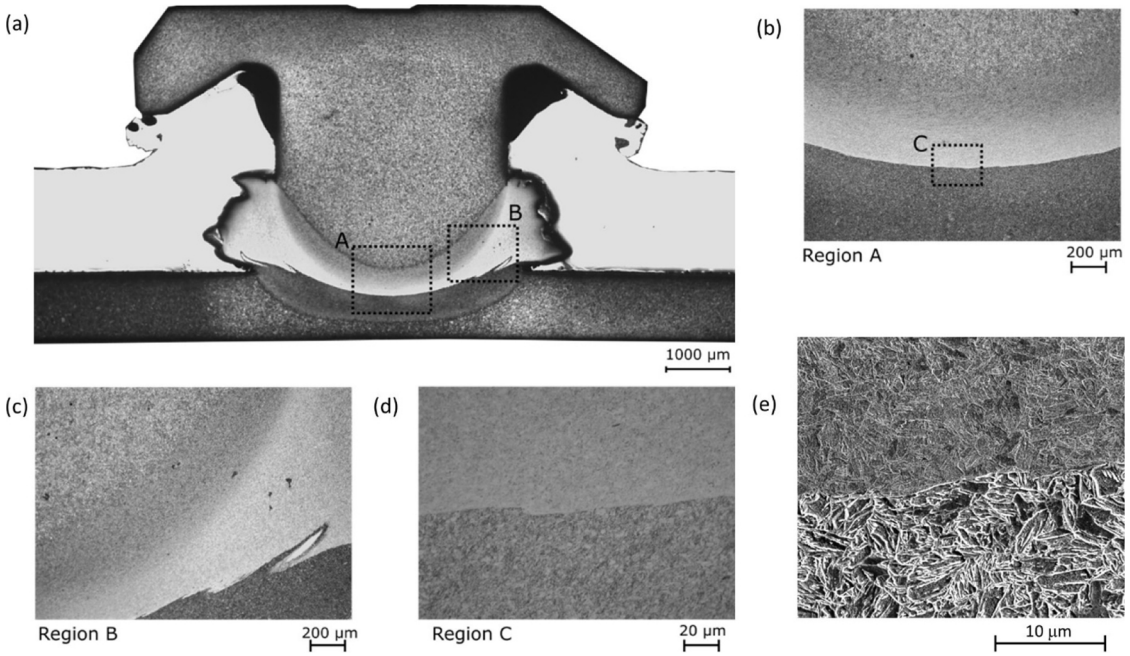

Fig. 6. Friction element weld of 6005-T5 aluminum and Usibor 1500 microstructure: (a) macrograph; (b) high magnification of joint interface within region A; (c) high magnification of swirl within region B; (d) high magnification of region C; (e) SEM of joint interface.

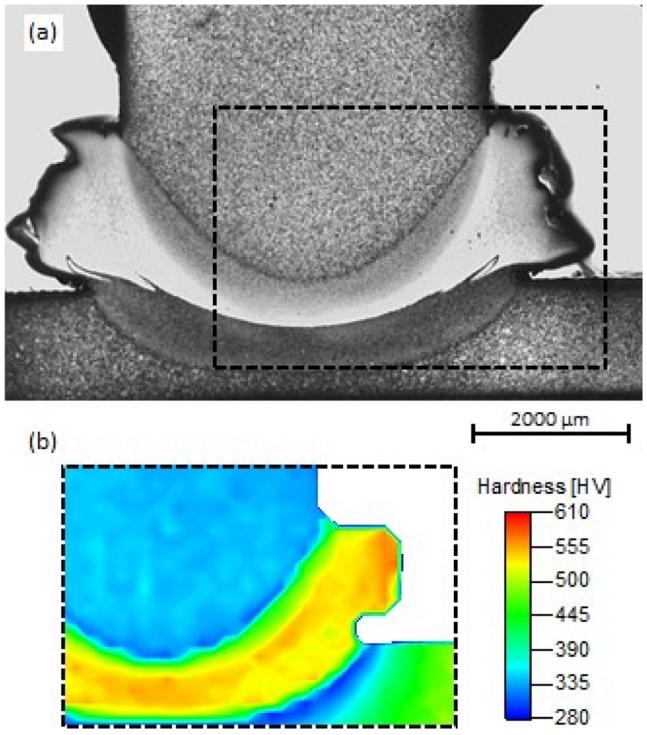

Fig. 7. (a) Macrograph of the friction element joint with dashed box to represent the indented region; (b) microhardness map of the friction element joint.

3.3. Resistance spot welding/Friction element welding microstructural characterization

The friction element weld macrograph of aluminum 6005-T5 to Usibor 1500 stack is depicted in Fig. 8. Different thermally affected regions can be observed as a consequence of the combined effect of the friction element weld on to the Usibor stack. Region A in Fig. 8a depicts a new heat affected zone created on the fusion zone of the resistance spot weld as well as another created on the region adjacent to the weld nugget. Region B in Fig. 8a corresponds to the central region of the weld. Different regions can be identified there: at the interface of the friction element and the Usibor nugget there are two regions which experienced grain refinement (one on each material). This grain refinement effect is a consequence of dynamic recrystallization occurring during friction element welding. During friction element welding a significant amount of plastic deformation is generated, which associated with an increase in temperature promotes the dynamic recrystallization phenomena. Further into the nugget of the Usibor weld it can be observed that some recrystallization occurred in the fusion zone of the Usibor. This recrystallization was promoted by the temperatures above Ac_3 experienced by this region during the friction element welding. Moreover, further into the weld centerline the temperature was still above the Ac_3 temperature promoting full austenitization of the material. The cooling rates experienced in this region were still high enough to promote a fully martensitic microstructure.

Scanning electron microscopy of the different regions of the welded joints provided a clearer notion of the microstructures obtained. Fig. 8d depicts the interface between the friction element weld and the Usibor nugget. A significant grain size reduction is observed in the Usibor nugget owing to the dynamic recrystallization process, which occurred during friction element welding. Additionally, the microstructure in the friction element is composed of a fine grain, near-equiaxed martensitic structure. Of special interest is the layer formed in between the friction element and the Usibor, depicted in Fig. 8d with a thickness of approximately 1–5 μm.

Energy dispersive X-ray spectroscopy (XEDS) was performed and it revealed that an aluminum-rich phase formed in between the two materials (Fig. 9). Formation of such phase is predicted by the Al-Fe phase diagram. According to the Al-Fe phase diagram, the Al-rich phase is an ordered cubic phase that accepts a compositional range of 51–73 at% Fe; therefore, the aluminum composition within the analyzed region is expected to vary. The EDS compositional data also

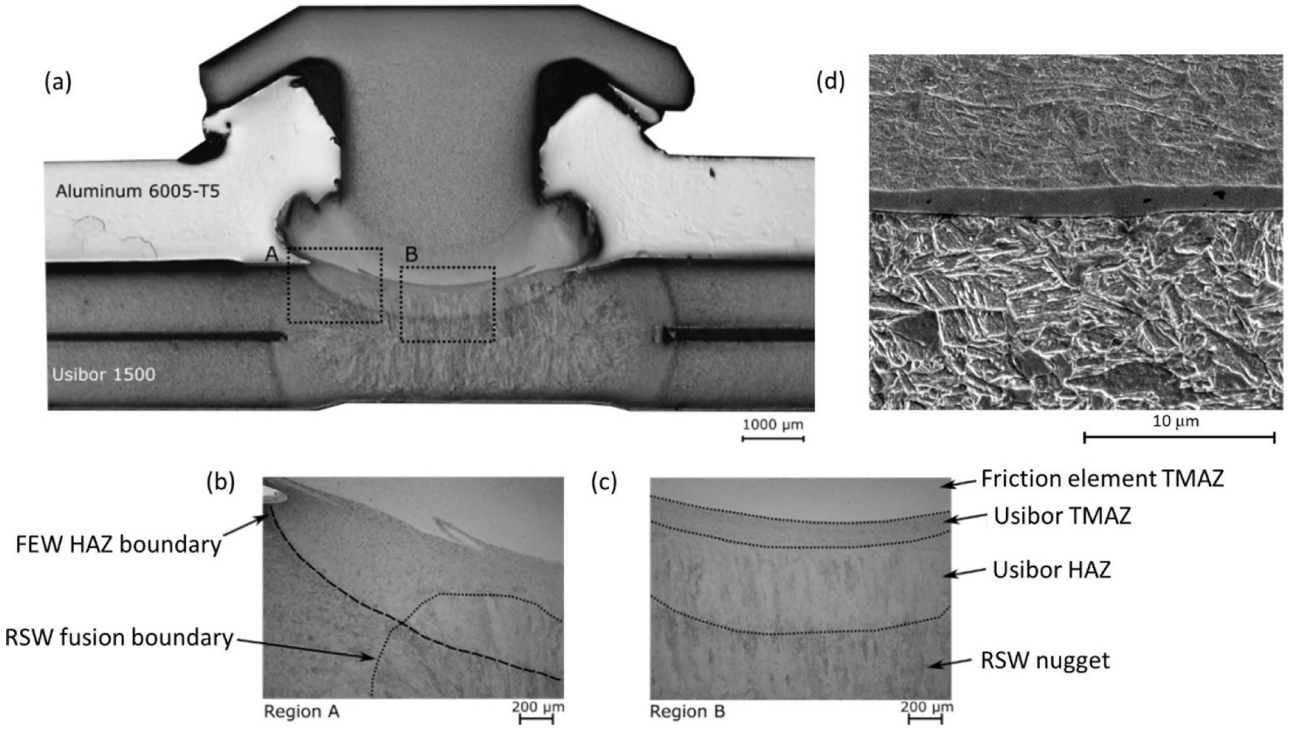

Fig. 8. Multi-process resistance spot welding/friction element welding joint microstructure: (a) macrograph; (b) high magnification of region A; (c) high magnification of region B; (d) SEM of Al-rich layer at joint interface.

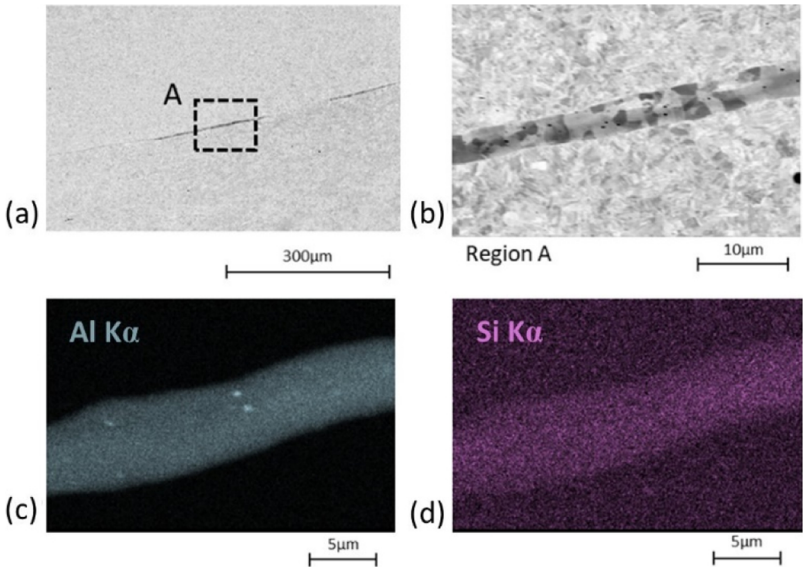

Fig. 9. SEM of Al-rich layer at resistance spot weld/friction element weld interface taken at 7.2 keV: (a) backscatter macrograph; (b) high magnification of region A; (c) EDS Al map; (d) EDS Si map.

provides evidence to the source of aluminum and silicon within the intermetallic layer. According to Borsetto et al. (2009). The aluminum-silicon coating on Usibor 1500 steel is composed of aluminum with 10–13% silicon. The compositional ratio of aluminum to silicon within the layer, 43.3 at% Al to 5.8 at% Si, is consistent with the ratio within the aluminum-silicon coating on the Usibor 1500 steel. A nanohardness map of the region is depicted in Fig. 10. The Al-rich layer had a lower hardness when compared to the friction element and the resistance spot weld fusion zone (Usibor 1500).

The joining mechanisms in friction element welding arise from the intrinsic characteristics of the process. The combined action of high temperature and cleaning effect, created by the friction, between the friction element material and the Usibor, creates a rigid metal bond by diffusion. Moreover, when the temperature decreases there is a shrinkage of the material along the axial direction, which created a force-lock between the friction element used and the Usibor.

The effect of the friction element welding on the hardness profile of the Aluminum 6005-T5/Usibor stack is significant when compared to the as-welded Usibor stack observed in Fig. 11. For proper comparison, the hardness scale was kept the same for all hardness maps presented, and no hardness measurements on the aluminum side were measured due to the significant difference in hardness. It is clear a significant increase in the hardness values occur at and near the joined interface between the Usibor and the friction element material. This increase in hardness is due to two distinct features: the first is the dynamic recrystallization phenomena, which promotes grain refinement and therefore an increase in hardness; the second is the fast cooling rate after welding, which is ensured by the large volume of material acting as a heat sink, thus allowing the austenitized

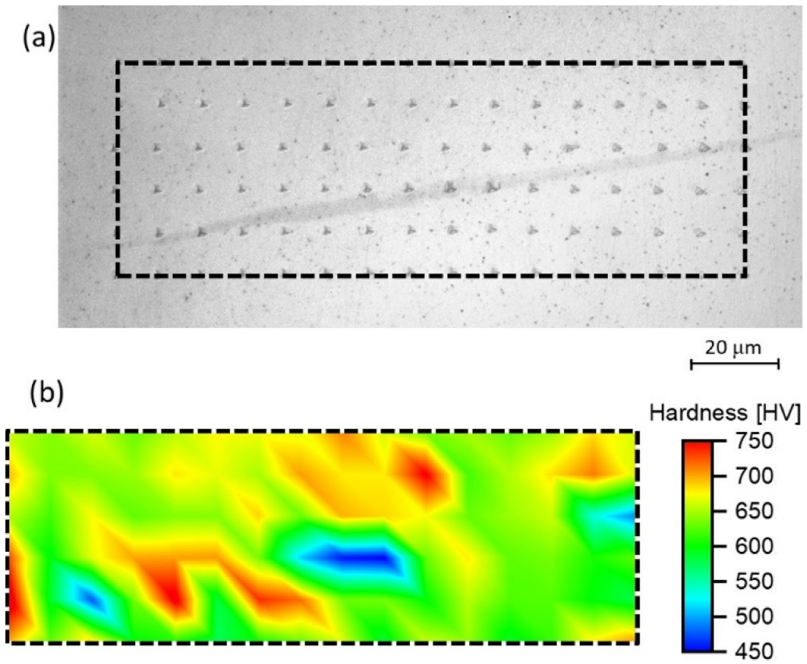

Fig. 10. (a) Micrograph of the Al-rich layer at the multi-process resistance spot weld/friction element weld joint interface with dashed box to represent the indented region; (b) nano-hardness mapping of Al-rich layer at the joint interface.

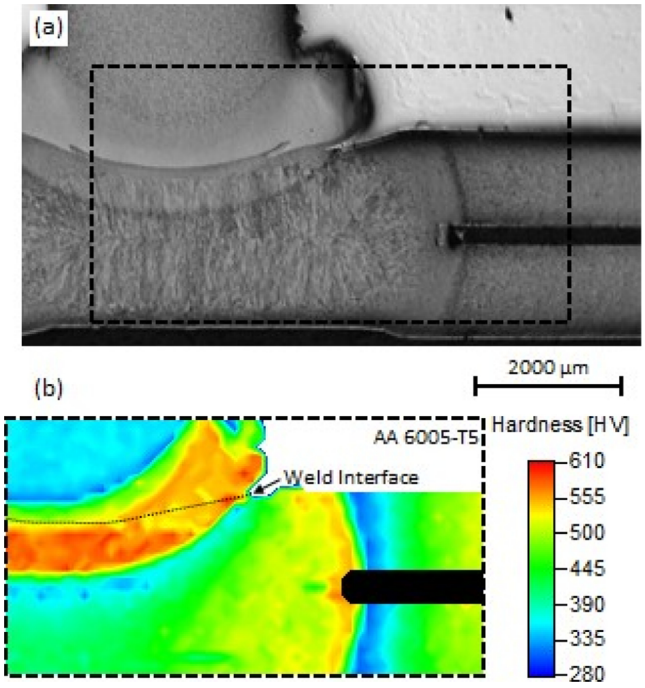

Fig. 11. Macrograph of the multi-process resistance spot weld/friction element weld joint with dashed box to represent the indented region; (b) microhardness mapping of the resistance spot weld/friction element weld joint.

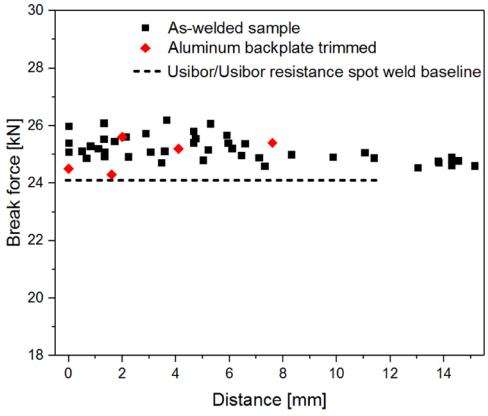

Fig. 12. Effect of offset distance on the breaking force during tensile shear testing when the Usibor/Usibor resistance spot welded joint in multiple stack is solicited. The dashed line represents the average break force for the Usibor/Usibor resistance spot weld.

material to become fully martensitic. This cooling rate effect is especially evident when analyzing the hardness maps presented in both Figs. 7b and 11. In the joint created between the aluminum and the resistance spot welded Usibor (Fig. 1) the mass of material is significantly higher than when joining only the aluminum to one sheet of Usibor. Therefore, the cooling rate will be significantly higher in the first case, giving rise to a significant increase in hardness.

3.4. Mechanical characterization

In order to evaluate the effect of offset distance on the mechanical properties of the multi-stack joints, shear tensile tests were performed. As previously mentioned, the tensile testing performed on the multiple stacks was done to evaluate the effect of offset distance on the break force when either the resistance spot weld or the friction element weld part of the joint was stressed (Fig. 2c and d, respectively). Moreover, to

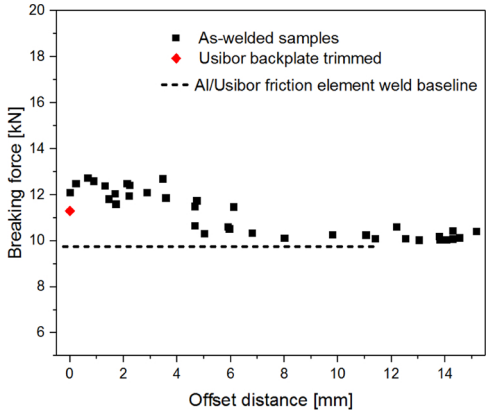

Fig. 13. Effect of offset distance on the breaking force during tensile shear testing when the Aluminum/Usibor friction element joint was solicited.

have a baseline to guide the understanding of this offset distance effect the Usibor/Usibor resistance spot weld, and the Aluminum/Usibor friction element weld was also tested (Fig. 2a and b, respectively). These baselines are presented in Figs. 12 and 13 as dash lines.

From the analysis of the effect of break force versus offset distance presented in both Figs. 12 and 13 (corresponding to the testing performed on the Usibor/Usibor resistance spot weld after friction element welding of the Usibor plates to the Aluminum and on the Usibor/Aluminum friction element welds after resistance spot welding of the Usibor plates, respectively), it can be seen that the most significant difference occurs of the Usibor/Aluminum joints. The break force for the resistance spot welded joint after friction element welding ranges between 24 and 26 kN, a slight decrease in the break force is observed when the offset distance increases. On the other hand, the same does not occur for the Usibor/Aluminum friction element welds after resistance spot welding of the Usibor plates. In this case the breaking force varies between 10 and 13 kN, with the break force decreasing as the offset distance increases. In both cases, all the results obtained are above the baseline obtained from the single welds of Usibor/Usibor by resistance spot welding and Usibor/Aluminum by friction element welding.

It is of special interest to note that depending on the offset distance, the fracture mode changes. When the Usibor/Usibor resistance spot weld in the multiple stack (Fig. 12) has an offset distance of the friction element weld regarding the center of the nugget of up to 7 mm, interfacial failure occurred. Above 7 mm, the fracture mode changes to double-pull out failure, which was also experienced by the resistance spot welded samples used for baseline comparison. The fracture surface of an interfacial failure is shown in Fig. 14. It can be seen that the topography of this fracture surface follows the rotational movement of the friction element welding process. The dimple size varies within the fracture surface: at the relatively smooth places shown in region A (Fig. 14b) a smaller dimple size is observed, whereas on the remaining regions the dimple size is significantly larger (Fig. 14c).

On the other hand, when the Aluminum/Usibor friction element weld is tested on the multi-stack joint, interfacial failure is observed when the offset distance is 3 mm. Above that value, partial thickness failure with button pull occurs, which is similar to what happens for the Aluminum/Usibor friction element welds used as baseline. A fracture surface of a partial thickness failure with button pull is depicted in Fig. 15. In the overview of the fracture surface (Fig. 15a), two distinct regions can be observed: regions A and B. In the former, several microcracks can be observed and these propagate transgranularly (Fig. 15b) whereas in the later, ductile-like surfaces with several dimples are observed (Fig. 15c).

Typically, button pullout failure is preferable due to a higher associated plastic deformation and energy absorption (Pouranvari and Marashi, 2013). As described by Radakovic and Tumuluru (2008) when

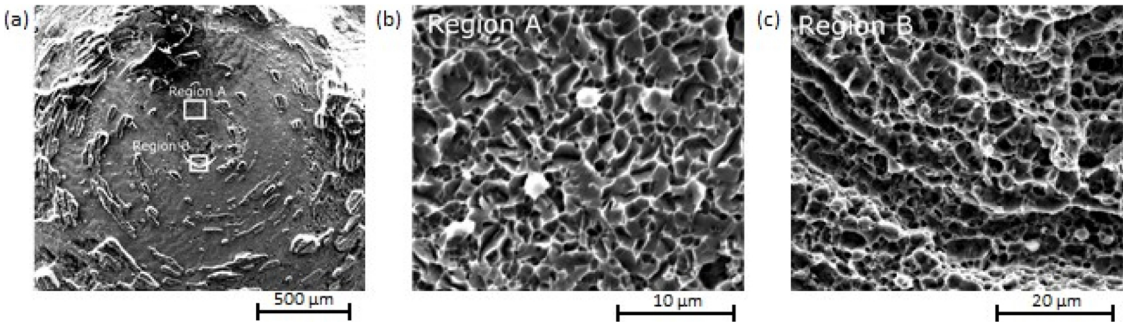

Fig. 14. Fracture surface of resistance spot welded joint with interfacial failure: (a) SEM macrograph; (b) high magnification of region A; (c) high magnification of region B.

button pull out failures occur, the specimens tend to undergo a significant rotation along an axis perpendicular to the load direction, whereas a small amount of rotation occurs when the welded samples fail in a interfacial way. In the present work, it was observed that when interfacial failure modes occur the degree of rotation was almost non-existent. In order to understand if the failure mode was caused by a geometrical constraint, namely the back plates, which compose the multiple stacks but are not being pulled during tensile shear testing, new tensile tests were performed. In these new tensile tests, the back-plates were trimmed to understand if there was any stabilization effect occurring which the welds were prevented from rotating and therefore exhibited pull out failure. A schematic representation of trimmed sheets is presented in Fig. 16.

For the Usibor/Usibor resistance spot welding test in the multiple stack joint, no significant differences were found (red spots on Fig. 12) when comparing with the non-trimmed specimens. However, for the Aluminum/Usibor friction element weld in the multi-stack joint, when the Usibor backplate was removed partial thickness failure with button pull was observed (Fig. 17). Additionally, the break force of the joints slightly decreased when compared with the non-trimmed specimens (red spots on Fig. 13). Due to lack of material, only two joints with the Usibor backplate trimmed could be tested. However, it is clear the effect of the Usibor backplate on the break force and failure mode of the welds.

The high rigidity of the Usibor backplate constrains the Aluminum/Usibor friction element weld in the multi-stack. This mechanical stabilization effect prevents significant rotation of the weld and therefore no button pull out failure occurs. As a result, the break force of the joint increases. The effect of the Aluminum backplate on the Usibor/Usibor resistance spot welded joints in the multi-stack is negligible due to the significant difference in strength between the aluminum plate and the Usibor. Since the aluminum is significantly softer, no mechanical stabilization effect occurs. When the offset distance is sufficiently high, above 6 mm, this stabilization effect is negligible, and the joints fails similar to those used for baseline comparison.

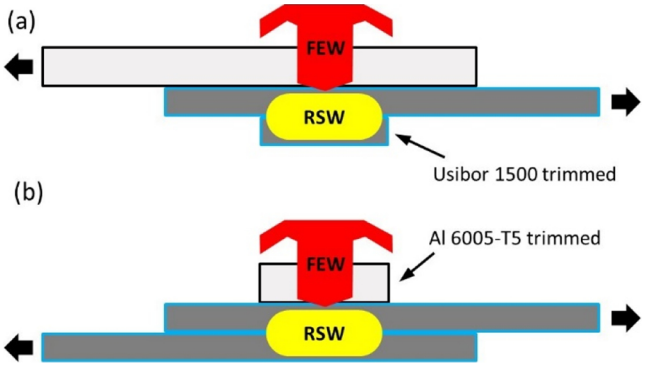

Fig. 16. Schematic representation of trimmed tensile shear tests performed: (a) Usibor 1500 trimmed for friction element welding tensile testing; (b) Aluminum 6005-T5 trimmed for resistance spot welding tensile testing.

4. Conclusions

The effect of the offset distance between a friction element weld made of Aluminum 6005-T5 and a resistance spot welded stack of high strength steel Usibor 1500 was microscopy techniques and mechanical testing. The following major conclusions can be drawn:

- The thermomechanical history imposed on the materials by both joining techniques, resistance spot welding and friction element welding, created complex joint microstructures including fusion zone, severely deformed zone and several heat affected zones, where the final microstructure and hardness throughout the joints were mostly determined by the attained peak temperatures, holding time and

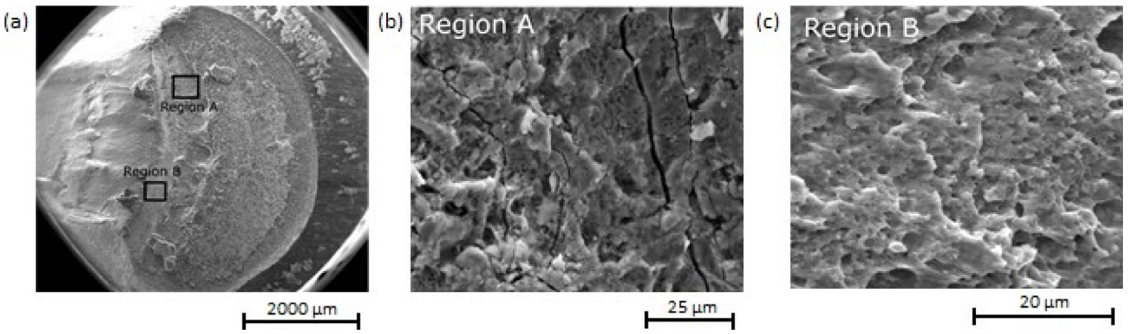

Fig. 15. Fracture surface of friction element welding joint with partial thickness failure and button pull: (a) SEM macrograph; (b) high magnification of region A; (c) high magnification of region B.

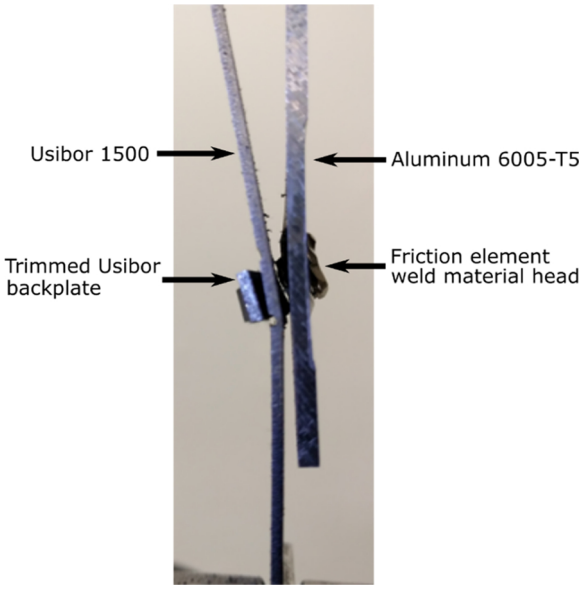

Fig. 17. Partial thickness failure with button pull failure in the Aluminum/Usibor friction element weld in the multi-stack joint.

subsequent the cooling conditions. These sub-regions consisted primarily of fresh and tempered martensite with a wide range of harness.

- Tensile shear testing confirmed that the quase-static mechanical properties of the multi-stack joints always exceeded those of each one of the single process joints. A change in failure mode was observed in the resistance spot welded tensile shear tests, below 7 mm join offset interfacial fracture occurred, while above 7 mm offset pullout fracture occurred.

- The offset distance between the resistance spot nugget and the friction element was observed to affect the failure mode of the joints, with interfacial failure occurring for smaller offsets and double pull out for higher offsets.

Acknowledgements

The authors acknowledge the support of Kerem Ipekbayrak from EJOT USA during the friction element welding experiments and Guilherme Abreu Faria from The Ohio State University for the EDS work used to identify the Al-rich region found between the FEW/Usibor materials. JPO acknowledges Fundação para a Ciência e Tecnologia (FCT) for its financial support through the project UID/EMS/00667/2019.

References

Boriwal, L., Sarviya, R.M., Mahapatra, M.M., 2017. Failure modes of spot welds in quasi – static tensile – shear loading of coated steel sheets. ScienceDirect 4, 3672–3677.

Borsetto, F., Ghiotti, A., Bruschi, S., 2009. Investigation of the high strength steel Al-Si coating during hot stamping operations. Key Eng. Mater. 410–411, 289–296. https://doi.org/10.4028/www.scientific.net/KEM.410-411.289.

Eller, T.K., Greve, L., Andres, M., Medricky, M., Meinders, T., van den Boogaard, T., 2015. Identification of plasticity model parameters of the heat-affected zone in resistance spot welded martensitic boron steel. Key Eng. Mater. 639, 369–376. https://doi.org/10.4028/www.scientific.net/KEM.639.369.

Ighodaro, O.L., Biro, E., Zhou, Y.N., 2016. Comparative effects of Al-Si and galvannealed coatings on the properties of resistance spot welded hot stamping steel joints. J. Mater. Process. Technol. 236, 64–72. https://doi.org/10.1016/j.jmatprotec.2016.03.021.

Khan, M.I., Kuntz, M.L., Biro, E., Zhou, Y., 2008. Microstructure and mechanical properties of resistance spot welded advanced high strength steels. Mater. Trans. 49, 1629–1637. https://doi.org/10.2320/matertrans.MRA2008031.

Maiwald, M., Thiem, J., 2012. Joining without a pilot hole using friction welding. Dev. Join. Technol. 5, 10–16. https://doi.org/10.1365/s38312-012-0045-0.

Pouranvari, M., Marashi, S.P.H., 2013. Critical review of automotive steels spot welding: process, structure and properties. Sci. Technol. Weld. Join. 18, 361–403. https://doi.org/10.1179/1362171813Y.0000000120.

Radakovic, D.J., Tumuluru, M., 2008. Predicting resistance spot weld failure modes in shear tension tests of advanced high-strength automotive steels. Weld. J. 87, 96S–105S.